ResearchGate

See discussions, stats, and author profiles for this publication at: https://www.researchgate.net/publication/258671602

Statistical study of the equatorial F2 layer critical frequency at Ouagadougou during solar cycles 20, 21 and 22, using Legrand...

Article *in* Journal of Space Weather and Space Climate · November 2012

DOI: 10.1051/swsc/2012019

CITATIONS
5

READS
13

2 authors:

Ouattara Frédéric
université de Koudougou
53 PUBLICATIONS **125** CITATIONS

SEE PROFILE

Christine Amory-Mazaudier
Pierre and Marie Curie University - Paris 6
159 PUBLICATIONS **1,409** CITATIONS

SEE PROFILE

Some of the authors of this publication are also working on these related projects:

Project International Electrojet Equatorial Year View project

Project International heliophysical Year View project

All content following this page was uploaded by Ouattara Frédéric on 07 March 2014.

The user has requested enhancement of the downloaded file. All in-text references underlined in blue are added to the original document and are linked to publications on ResearchGate, letting you access and read them immediately.

J. Space Weather Space Clim. 2 (2012) A19
DOI: 10.1051/swsc/2012019
© Owned by the authors, Published by EDP Sciences 2012

Statistical study of the equatorial F_2 layer critical frequency at Ouagadougou during solar cycles 20, 21 and 22, using Legrand and Simon's classification of geomagnetic activity

Frédéric Ouattara[1,2] and Christine Amory-Mazaudier[2,*]

[1] Université de Koudougou, BP 376, Koudougou, Burkina Faso
[2] Laboratoire de Physique des Plasmas/UPMC/Polytechnique/CNRS, 4 avenue de Neptune, 94107 Saint-Maur-des-Fossés, France
*corresponding author: e-mail: christine.amory@lpp.polytechnique.fr

Received 20 February 2012 / Accepted 19 November 2012

ABSTRACT

This paper presents the statistical analysis of the diurnal variations of the F layer at the equatorial station of Ouagadougou (Lat: 12.4° N; Long: 358.5° E; dip: 5.9°) from 1966 to 1998 (=> ~11 680 days). We consider three main factors of variability: (1) the season (spring, summer, autumn and winter), (2) the phase of the sunspot cycle (ascending, maximum, descending and minimum) and (3) the geomagnetic activity classified by Legrand and Simon in four groups: slow solar wind, high solar wind streams, fluctuating solar wind and shock activity. We easily identify the influence of the solar wind speed and shock activity on the diurnal pattern of the F layer. Shock and recurrent activities tend to enhance or diminish the morning or afternoon maximum of the F2 layer critical frequency. The difference of the diurnal foF2 variation during the increasing and decreasing phases of the sunspot solar cycle is explained by different solar wind regimes. The slow solar wind dominates during the increasing phase of the sunspot cycle and the fluctuating solar wind dominates during the decreasing phase of the sunspot cycle. This paper demonstrates that it is possible using a large database, to bring up significant morphologies of the diurnal variation of the foF2 critical frequency as a function of (1) different solar events such as quiet solar wind, fluctuating wind, recurrent high stream wind and Coronal Mass Ejections (CMEs); (2) solar cycle phases and (3) seasons. It is an approach directly connecting the critical frequency of the F2 layer to the solar parameters.

Key words. ionosphere – geomagnetic activity – solar activity – solar CME – solar coronal hole

1. Introduction

Since the first sounding of the ionosphere in 1926 by Breit & Tuve (1926), many studies have been performed on the variability of the F layer. It is well known that the F layer depends on: (1) the sunspot solar cycle (Phillips 1947; Forbes et al. 2000; Forbes et al. 2000; Rishbeth & Mendillo 2001; Pancheva et al. 2002), (2) the Sun-Earth relative position at the origin of the seasonal variation, and equinoctial maxima (Lal 1992, 1997, 1998; Arauje-Pradere 1997; Rishbeth et al. 2000; Zou et al. 2000) and (3) the solar wind speed (Legrand & Simon 1989; Lotko 1989; Simon & Legrand 1989; Lal 1997, 1998; Ouattara 2009a; Ouattara et al. 2009) and shock activity (Ouattara 2009b; Ouattara et al. 2009). Solar wind speed and shock activity are the main sources of geomagnetic activity. Coupling processes between the ionosphere and the underlying atmosphere also play an important role in solar cycle, geomagnetic activity and variations of altitude, latitude, longitude, local time and season of the low latitude ionosphere (Ren et al. 2009). The equatorial ionosphere variability depends on its electric field's day-to-day variability (Manoj et al. 2008) due on one hand to the wind forced field (Scherliess & Fejer 1999) and on the other hand to the penetrating electric fields (Huang et al. 2005; Nicolls et al. 2007). One can distinguish two main physical processes generating large-scale electric field which strongly influence low latitudes: (1) the prompt penetration (Vasyliunas 1970) and (2) the disturbance dynamo effects (Blanc & Richmond 1980; Fejer et al. 2007; Huang et al. 2007; Fejer 2011). All these coupling processes are related to the three main chosen factors of variability: the solar cycle, the season and the geomagnetic activity (shock and solar wind effects).

In this paper, we analyse 32 years (1966–1998, solar cycle 20, 21 and 22) of F2 critical frequency data at the equatorial station of Ouagadougou, Burkina Faso (lat: 12.4° N; long: 358.5° E; dip: 1.45°). We take into account the influences of the Sun-Earth relative position, sunspot activity, solar wind speed and shock activity to classify the data, in order to understand and predict the shape of the mean diurnal variation of the F2 layer. Such a study is only possible when there is a large existing continuous recording database. This is the case for the Ouagadougou station. The topic of this paper is to establish statistically typical morphologies of the foF2 variability. This study is part of the programme Sun-Earth integration studies (Amory-Mazaudier et al. 2006) in the framework of the International Heliophysical Year (http://ihy2007.org).

This paper is composed of five sections. Section 2 describes the data analysis. Sections 3 and 4 describe the main characteristics of the data. In Sect. 5, we discuss our results.

2. Data analysis

To analyse the data we use the following factors of variability:

1. The season: spring, summer, autumn and winter.
2. The sunspot number: we distinguish four parts: the minimum phase (years with the sunspot number $Rz < 20$),

This is an Open Access article distributed under the terms of Creative Commons Attribution 3.0 Unported License

the increasing phase (years with $20 \leq Rz \leq 100$), the maximum phase (years with $Rz > 100$) and the decreasing phase (years with $100 \geq Rz \geq 20$).

3. The solar wind speed: by analysing solar and geomagnetic activity over a long period (11 solar cycles), Legrand & Simon (1989) and Simon & Legrand (1989) divided solar wind into three parts: (a) slow solar wind due to solar wind coming from the solar heliosheet, (b) recurrent winds that are coming from coronal holes and (c) fluctuating winds that are produced by the fluctuation of the heliosheet.
4. The shock activity: this activity is due to CMEs (see Legrand & Simon 1989 and Simon & Legrand 1989).

These authors distinguished four classes of solar inputs (slow solar wind, recurrent solar wind, fluctuating solar wind and CMEs). Ouattara & Amory Mazaudier (2009) recently validated their results using in situ satellite measurements of the solar wind.

The four geomagnetic classes determined by Legrand & Simon (1989) are:

1. quiet magnetic activity due to slow solar wind;
2. recurrent activity related to high wind streams coming from coronal holes;
3. shock events with Sudden Storm Commencements (SSC) caused by Coronal Mass Ejections (CMEs);
4. fluctuating activity that includes all cases of which the mechanisms cannot be clearly identified. This class does not represent the signature of a particular solar event as it amalgamates all the cases that are not classified in the three previous classes.

In the past, the geomagnetic activity was classified in quiet magnetic periods with the three-hourly $Kp < 2+$, and magnetic disturbed periods with the three-hourly $Kp > 3$. In the present study we analyse the signature of particular strong geo-effective events (CMEs and high speed solar wind streams) that have daily Aa indices greater than 40 nT. The magnetic quiet period, defined in this study by daily Aa smaller than 20 nT, corresponds roughly to the previous classification of magnetic quiet days with $Kp < 2+$. In this study, the influence of the sunspot cycle is taken into account by considering the four solar cycle phases (minimum, increasing, maximum and decreasing).

Table 1 provides the summary of the classification based on the two components of the solar magnetic field. The closed magnetic field is highlighted by the sunspot cycle (toroidal component) and the open field (poloidal component) is expressed by the solar winds.

Table 2 gives the years for each sunspot cycle phase.

This classification leads to 64 classes: 4 seasons × 4 solar cycle intensity × 4 [solar wind (3) and shock activity (1)] = 64.

The database used permits us to take into account three facts:

1. The three considered solar cycles (20, 21, 22) have their maximum amplitude $Rz > 100$;
2. The variability of the critical frequency of the F2 layer (foF2) is small for the same phase from one solar cycle to another except for the increasing phase of solar cycle 20 (see Fig. 3 of Ouattara et al. 2009).
3. The critical frequency foF2 does not present long-term variation during the period analysed (Ouattara et al. 2009).

Taking into account these facts, we can analyse the average occurrence of each class over the three solar cycles together.

The hourly foF2 values for a given geomagnetic class of activity ($\mathrm{foF2}^{\mathrm{Hourly}}_{\mathrm{Geomag}}$) for the period 1966–1998 are determined using the following Eq. (1):

$$\mathrm{foF2}^{\mathrm{Hourly}}_{\mathrm{Geomag}} = \frac{\sum_{i=1}^{Nc} \mathrm{foF2}^{\mathrm{Hourly}}_{\mathrm{Cycle}}}{Nc}. \quad (1)$$

In this equation, $\mathrm{foF2}^{\mathrm{Hourly}}_{\mathrm{Cycle}}$ is the hourly mean foF2 value for the considered solar cycle phase and Nc is the number of solar cycle phases involved in the period 1966–1998. For this period, $Nc = 11$. Eleven is the sum of the two (2) minimum phases, the three (3) increasing phases, the three (3) maximum phases and the three (3) decreasing phases. From Table 2, it can be seen that for our period involved, there are three solar increasing phases, three solar maximum phases, three solar decreasing phases and two solar minimum phases because the minimum 1964 is not involved in the database period. By using Eq. (1) we determine the 24h mean values of foF2 for each type of geomagnetic class by considering the entire series of 11 229 days. Daily geomagnetic activity is evaluated by using pixel diagrams (see Legrand & Simon 1989; Simon & Legrand 1989; Ouattara & Amory Mazaudier 2009). The 11 229 days correspond to all the days of the 32 years minus the days of the first five months of the year 1966 and the days of the last 10 months of the year 1998.

For the solar cycle impact evaluation, the mean hourly foF2 value of a solar cycle phase ($\mathrm{foF2}^{\mathrm{Hourly}}_{\mathrm{Cycler}}$) is calculated using Eq. (2):

$$\mathrm{foF2}^{\mathrm{Hourly}}_{\mathrm{Cycle}} = \frac{\sum_{j=1}^{Ny} \mathrm{foF2}^{\mathrm{Hourly}}_{\mathrm{Year}}}{Ny}. \quad (2)$$

In this equation, $\mathrm{foF2}^{\mathrm{Hourly}}_{\mathrm{Year}}$ corresponds to the mean hourly foF2 value of the considered year and Ny is the number of years involved in the considered solar cycle phase. The number of years per solar cycle phase can be obtained by counting the number of years of each solar cycle phase shown in Table 2.

To determine the mean hourly foF2 value of the considered year ($\mathrm{foF2}^{\mathrm{Hourly}}_{\mathrm{Year}}$), one must use Eq. (3):

$$\mathrm{foF2}^{\mathrm{Hourly}}_{\mathrm{Year}} = \frac{\sum_{k=1}^{Nm} \mathrm{foF2}^{\mathrm{Hourly}}_{\mathrm{Month}}}{Nm}. \quad (3)$$

$\mathrm{foF2}^{\mathrm{Hourly}}_{\mathrm{Month}}$ corresponds to the monthly hourly mean value of foF2 and Nm is the number of available months involved in the considered year. Except year 1966 that contains 7 months and the year 1998 which has only 2 months. The other years have 12 months of daily foF2 values.

Table 1. Different classes of variability.

Factors of variability		Number of classes
	Ecliptic plane/solar magnetic equator – Sun-Earth relative position	
Seasonal variation	Spring Summer Autumn Winter	4 classes
	Toroidal component of the solar magnetic field	
Sunspot variation (radiation UV, EUV)	$Rz < 20 \rightarrow$ minimum $20 \leq Rz \leq 100 \rightarrow$ increasing $Rz > 100 \rightarrow$ maximum $100 \geq Rz \geq 20 \rightarrow$ decreasing	4 classes
Shock event Shock activity	Aa indices and SSC Classification by Legrand & Simon (1989) Richardson et al. (2000) Shock related to CME 1 class	4 classes
	Poloidal component of the solar magnetic field	
Quiet magnetic activity	Slow solar wind speed 1 class	
Geomagnetic activity Recurrent activity	High solar wind streams from coronal holes 1 class	
Geomagnetic activity Fluctuating activity	Fluctuating solar wind all other cases 1 class	

Table 2. Years for each phase of the different solar sunspot cycles.

Phases of solar sunspot cycle	Minimum $Rz < 20$	Increasing $20 \leq Rz \leq 100$	Maximum $Rz > 100$	Decreasing $100 \geq Rz \geq 20$
20	1964	1966–1967	1968–1970	1971–1975
21	1976	1977–1978	1979–1982	1983–1985
22	1986	1987–1988	1989–1991	1992–1995

For the seasonal study, the monthly hourly mean values of foF2 ($\mathrm{foF2}^{\mathrm{Hourly}}_{\mathrm{Month}}$) are obtained by utilizing Eq. (4):

$$\mathrm{foF2}^{\mathrm{Hourly}}_{\mathrm{Month}} = \frac{\sum_{l=1}^{N\mathrm{d}} \mathrm{foF2}^{\mathrm{Hourly}}_{\mathrm{Day}}}{N\mathrm{d}}. \quad (4)$$

In this equation $\mathrm{foF2}^{\mathrm{Hourly}}_{\mathrm{Day}}$ is an hourly foF2 value for a geomagnetic class day and Nd is the number of geomagnetic class days involved in the month considered. As previously noted, each geomagnetic class day is determined by means of the pixel diagrams.

For our morphological analysis, we put in the foF2 graph error bars that express the square of the variance ($\sigma = \sqrt{V}$). The variance is expressed as: $V = \frac{\sum_{i=1}^{N} \left(\mathrm{foF2}_i - \overline{\mathrm{foF2}}\right)^2}{N}$ where $\overline{\mathrm{foF2}}$ is the foF2 mean value, $\mathrm{foF2}_i$ is a given hourly foF2 value previously computed and N is the number of a given computed hourly foF2.

3. Results

Figure 1 illustrates the mean diurnal foF2 variation for the winter season during sunspot maximum (Fig. 1a) and sunspot minimum (Fig. 1b) for the four classes of activity (quiet, recurrent, shock and fluctuating). From Figure 1a, it can be seen that the foF2 diurnal variation is similar for recurrent (red dashed line) and shock (red full line) classes, i.e. foF2 decreases from 00:00 LT to 04:00 LT for recurrent activity and for shock activity it decreases from 00:00 LT to 06:00 LT. After that, foF2 increases to reach its maximum value around 10:00 LT for recurrent activity and 11:00 LT for shock activity and then it slowly decreases until 20:00 LT and increases after that time.

The pattern of the two other classes of activity (quiet activity: blue full line and fluctuating activity: blue dashed line) is different from that of the recurrent and shock classes of activity. In fact, the diurnal variation of the F2 layer critical frequency exhibits a double shape: it decreases from 00:00 LT to 06:00 LT, increases and reaches its first maximum around 10:00 LT. This diurnal profile shows a second peak at 18:00 LT. The error bars cannot explain the difference between the different classes. foF2 morning maximum amplitude is greater for shock activity (14.67 MHz) than for the others (recurrent activity: 13.37 MHz, fluctuating activity: 12.68 MHz and quiet activity: 11.54 MHz). After 16:00 LT, the foF2 diurnal variation for the four classes has similar amplitude. During shock day activity, the peak density is higher than the diurnal mean average during sunspot maximum.

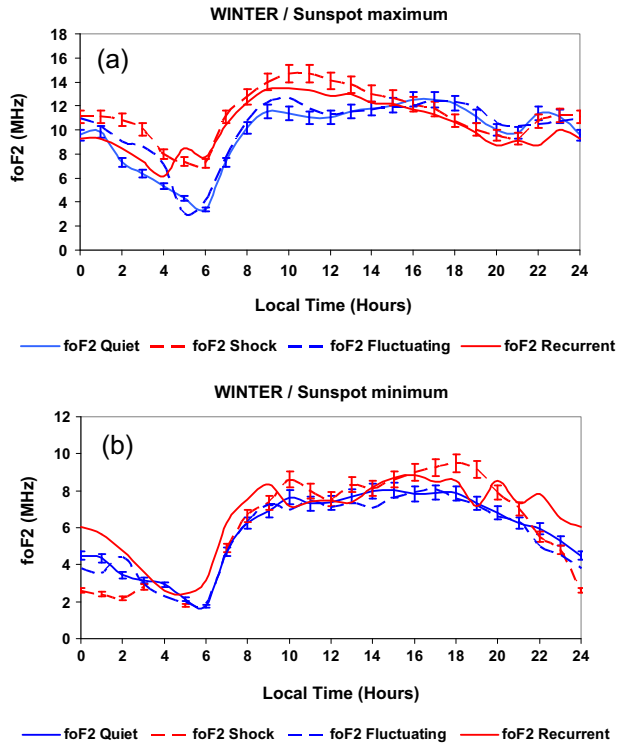

Fig. 1. foF2 variability for winter season during solar sunspot maximum (a) under quiet activity (blue full line), recurrent activity (red full line), shock activity (red dashed line) and fluctuating activity (blue dashed line). The bottom panel (b) corresponds to the solar minimum.

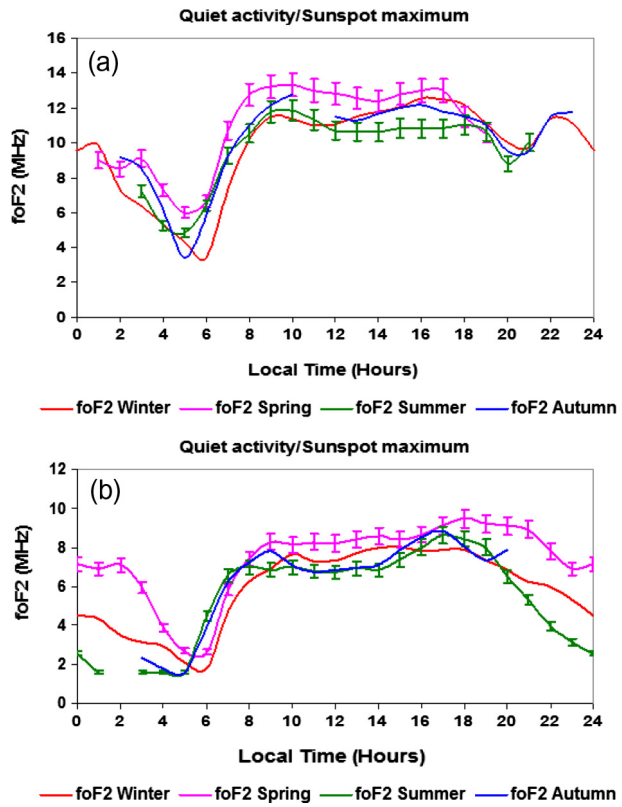

Fig. 2. foF2 variability during solar sunspot maximum (a) under quiet activity for winter season (red curve), spring season (pink curve), summer season (green curve) and autumn season (blue curve). The bottom panel (b) corresponds to sunspot minimum.

Both shock and recurrent activities provoke positive and negative storms; in fact, before 15:00 LT we have positive storm and after 15:00 LT we have negative storm.

In the following discussion, (1) $foF2_{shock}$ is expressed as $foF2_{sh}$, (2) $foF2_{recurrent}$ by $foF2_{rec}$, (3) $foF2_{fluctuating}$ by $foF2_{fluct}$ and (4) $foF2_{quiet}$ by $foF2_{q}$.

During the solar sunspot maximum, the following characteristics concerning the maxima can be seen during the winter season:

For the foF2 morning maximum: $foF2_{sh} > foF2_{rec} > foF2_{fluct} > foF2_{q}$
For the foF2 afternoon maximum: $foF2_{q} \sim foF2_{fluct} > foF2_{rec} \sim foF2_{sh}$

On the bottom panel of Figure 1, during the sunspot minimum, the main difference is seen from 05:00 LT to 09:00 LT where $foF2_{rec} > foF2_{fluct} \sim foF2_{sh} \sim foF2_{q}$ and at 10:00 LT and between 15:00 LT and 19:00 LT where $foF2_{sh} > foF2_{rec} > foF2_{fluct} \sim foF2_{q}$.

Figure 2 illustrates the mean diurnal variation of the F2 layer critical frequency for all seasons during sunspot maximum (Fig. 2a) and sunspot minimum (Fig. 2b) under magnetic quiet activity (red colour for winter, pink for spring, green for summer and blue for autumn). Both graphs show an increasing trend from morning to evening and are similar for all the seasons except for the summer season. During sunspot maximum, one can observe secondary maxima around 22:00 LT. During spring foF2 is highest (pink curve) for both sunspot maximum and minimum.

In the following discussion (1) $foF2_{spring}$ is expressed by $foF2_{sp}$, (2) $foF2_{autumn}$ by $foF2_{aut}$, (3) $foF2_{summer}$ by $foF2_{sum}$ and (4) $foF2_{winter}$ by $foF2_{win}$.

At sunspot maximum for quiet magnetic activity (slow solar wind), there is the following relationship between maxima:

Morning maxima : $foF2_{sp} > foF2_{sum} \sim foF2_{win} > foF2_{aut}$
Afternoon maxima : $foF2_{sp} > foF2_{win} > foF2_{sum} > foF2_{aut}$

At sunspot minimum for quiet activity, there is the following relation between the maxima (morning and afternoon) of foF2 -> $foF2_{sp} > foF2_{aut} > foF2_{sum} > foF2_{win}$.

Figure 3 characterizes the diurnal variation of foF2 for the four seasons under recurrent activity during sunspot maximum (Fig. 3a) and sunspot minimum (Fig. 3b). During sunspot maximum (Fig. 3a), the winter, autumn and spring curves exhibit the same pattern with a morning maximum around 09:00 LT and no afternoon maxima. During summer, there is no morning maximum.

The relation between the maxima is given by the following expression:

$$foF2_{aut} > foF2_{win} > foF2_{sum} > foF2_{sp}.$$

During sunspot minimum (Fig. 3b) the curves are different. During autumn the critical frequencies are very large compared to the three other seasons.

Figure 4 shows the foF2 variation during quiet magnetic activity for the four seasons. The top panel corresponds to the increasing phase and the bottom one to the decreasing phase.

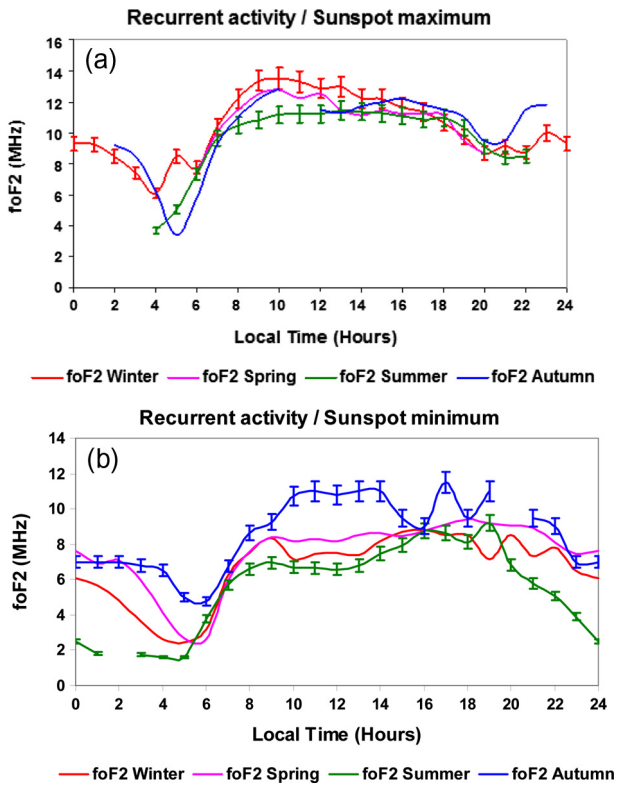

Fig. 3. foF2 variability for the different seasons, under recurrent magnetic activity, during sunspot maximum (a). The red curve corresponds to winter, the blue curve to autumn, the pink curve to spring and the green curve to summer. The bottom panel (b) is similar to the top one for sunspot minimum.

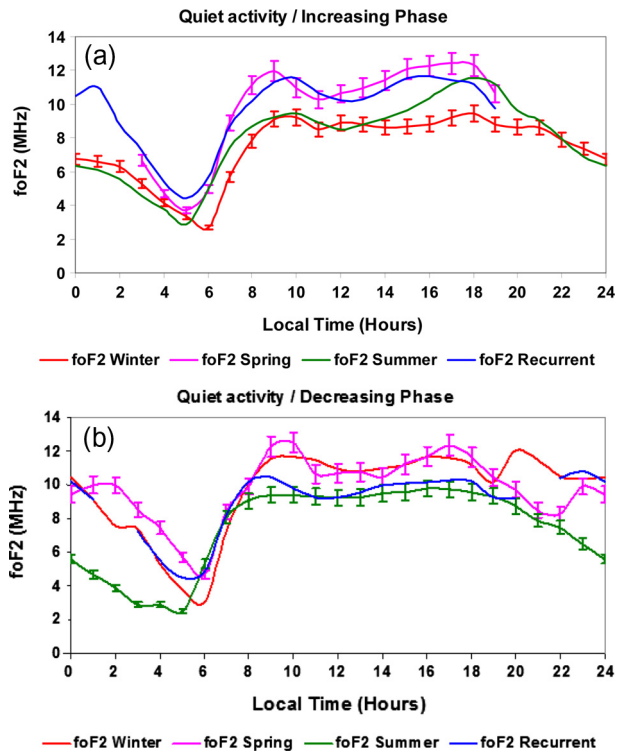

Fig. 4. foF2 for quiet magnetic activity during the increasing phase of the sunspot cycle (a) and the decreasing phase (b). The blue curve corresponds to autumn, the red one to winter and the pink and green ones respectively to spring and summer.

During the increasing phase (Fig. 4a), the foF2 variation is rather similar for all seasons with a morning maximum, a midday trough and an evening maximum.

One particular feature is observed during winter: the afternoon maximum (around 19:00 LT) is very high.

Concerning the mean amplitude of the foF2, there is the following relationship:

$$\mathrm{foF2}_{\mathrm{sp}} \sim \mathrm{foF2}_{\mathrm{aut}} > \mathrm{foF2}_{\mathrm{win}} \sim \mathrm{foF2}_{\mathrm{sum}}.$$

During the decreasing phase (Fig. 4b), the foF2 amplitude during summer and autumn seasons is smaller than the amplitude observed during winter and spring. Both panels a and b show an evening maximum around 20:00 LT.

Concerning the mean amplitude of the foF2, there is the following relation:

$$\mathrm{foF2}_{\mathrm{sp}} \sim \mathrm{foF2}_{\mathrm{win}} > \mathrm{foF2}_{\mathrm{aut}} \sim \mathrm{foF2}_{\mathrm{sum}}.$$

Figure 5 shows the foF2 variation under fluctuating activity for the four seasons during the increasing (Fig. 5a) and decreasing phases (Fig. 5b).

During increasing phase, all the seasons exhibit the same variation: morning maximum, midday trough and evening maximum. It is interesting to note that there is not any strong dispersion in the data.

Figure 5b shows large differences between winter and the other seasons that error bars cannot explain. The largest foF2 values are observed during spring before midday with maxima at midnight and around 9:00 LT. During autumn, there is an

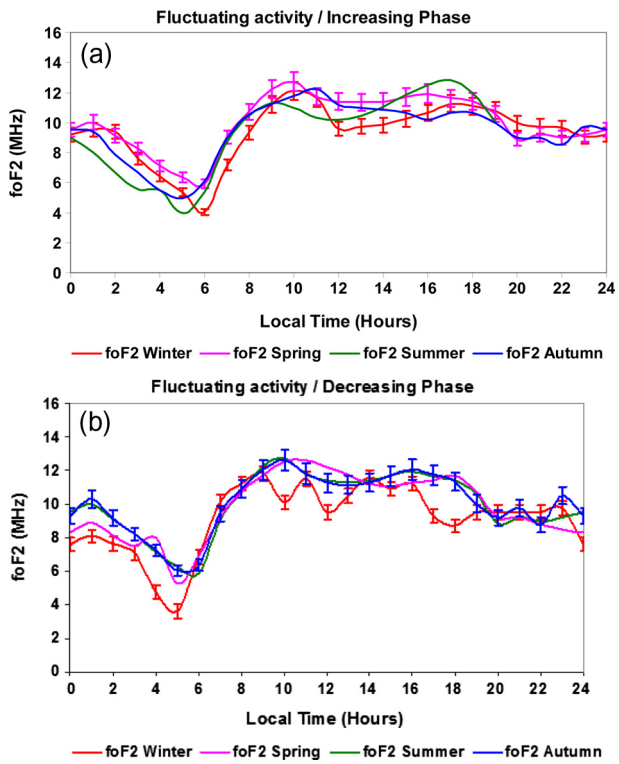

Fig. 5. foF2 variability under shock fluctuating geomagnetic activity during the sunspot increasing phase (a) and the sunspot decreasing phase (b). The blue curve corresponds to autumn, the red one to winter and the pink and green ones respectively to spring and summer.

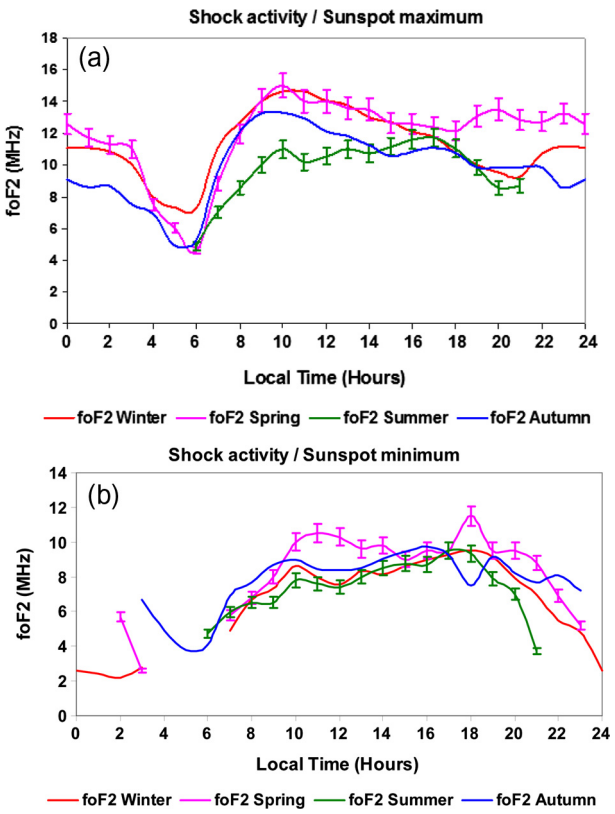

Fig. 6. foF2 variability under shock activity during solar sunspot maximum (a) and sunspot minimum (b), for winter season (red curve), spring season (pink curve), summer season (green curve) and autumn season (blue curve).

evening maximum around 21:00 LT. During summer, the foF2 variation exhibits a large plateau from 8:00 LT to 18:00 LT. During winter, the foF2 variation fluctuates. We must recall here that the class of fluctuating activity amalgamates all the cases that are not classified as quiet, shock or recurrent cases.

Figure 6 illustrates the foF2 variation for the four seasons under shock activity during sunspot maximum (Fig. 6a) and sunspot minimum (Fig. 6b). During sunspot maximum shock activity pattern is rather similar to recurrent activity pattern (Fig. 3a), with a strong morning maximum for three seasons (autumn, spring and winter). In summer the maximum is weak and occurs in the afternoon around 17:00 LT. The highest amplitude of the morning maxima is observed in spring and summer.

During sunspot minimum there is no clear pattern. The maximum amplitude of foF2 is observed in spring. The three other seasons exhibit similar variations.

4. Characteristics of the data

The morphological analysis of the 64 classes clearly shows that:

1. For all seasons during sunspot maximum, the recurrent and shock activities roughly exhibit similar patterns (Figs. 3a and 6a). During winter and for sunspot maximum, recurrent and shock activities produce positive storm effects in the morning and negative storm effects during the evening hours and at night (Fig. 1a). This coexistence of the two storm phases has also been obtained by Lu et al. (2001) during their simulation of the storm effect during the winter season in the northern hemisphere. This coexistence is a result of the complex dynamical and chemical interactions between charged particles and neutral gases (Lu et al. 2001). The main cause of negative storm is the increase of neutral molecular densities (Prölss 1987). The observed positive storm during winter conditions has been mentioned by Rishbeth (1989) and Burns et al. (1991, 1995). In winter, during sunspot maximum, F2 layer critical frequencies are greater for shock events than for recurrent events between 11:00 LT and 14:00 LT and from 20:00LT till 05:00 LT (see Fig. 1a).
2. F2 layer critical frequencies, under quiet magnetic condition (Figs 2a, 2b, 4a and 4b), for all sunspot cycle phases and all seasons, exhibit the same pattern: graph profiles present a morning maximum around 09:00 LT, and an evening maximum around 18:00 LT with a trough around midday.
3. Under quiet and fluctuating conditions (Figs. 2a, 2b, 4a, 4b, 5a and 5b, respectively), and whatever the season, quiet time foF2 (Figs. 2a, 2b, 4a and 4b) always exhibits the same pattern (morning and evening peaks with trough around midday) as the fluctuating time foF2 during the increasing phase of the sunspot cycle for all seasons (Fig. 5a). This is in sharp contrast with the decreasing phase, when there is a large difference between quiet shut foF2 (Figs 4b and 5b, respectively).
4. During sunspot minimum, F2 layer critical frequencies under shock and recurrent conditions (Figs. 3b and 6b) exhibit an unclear or a fluctuating pattern. There are similar observations for F2 layer critical frequencies under fluctuating conditions during the decreasing phase of the solar cycle (Fig. 5b).
5. F2 layer critical frequency for a similar season and under similar geomagnetic conditions maximizes during sunspot maximum and minimizes during sunspot minimum (see Figs. 1–4 and 6).
6. Under magnetic quiet conditions, both during sunspot maximum and minimum, the largest F2 critical frequencies are observed in spring (Figs. 2a and 2b).
7. During sunspot maximum and under recurrent conditions (Fig. 3a), the largest F2 critical frequencies are observed in winter. Autumn critical frequencies are greater than the spring ones and the summer critical frequencies are the smallest ones.
8. At solar minimum, for days under recurrent condition, winter values of foF2 are greater than the summer ones (Fig. 3b). This fact was previously observed by Araujo-Pradere (1997), Zou et al. (2000) and Rishbeth et al. (2000) during their research.

Tables 3a and 3b give for the sunspot maximum and during the four seasons, foF2 peak and trough values and timings. Tables 3a and 3b show that the quiet and fluctuating activities always highlight peaks in a morning and an evening and a trough around the midday. Recurrent activity (Tables 3a and 3b) shows a morning and an evening peaks and midday trough during the spring and the autumn. Shock activity (in both Tables 3a and 3b) highlights a morning and an evening peaks and the midday trough during the summer and the autumn. The same pattern is observed for the shock activity in the winter and the spring. In winter (Table 3a) the lowest value of foF2 morning peak is observed for quiet activity (11.51 MHz) and the highest for shock activity (14.67 MHz). In summer

Table 3. Characteristics of the observations of foF2, (a) for the sunspot maximum during winter and spring for the four classes of geomagnetic activity, and (b) for the sunspot maximum during summer and autumn for the four classes of geomagnetic activity.

	Winter						Spring					
	foF2 graph characteristics											
	Sunspot maximum											
	Morning peak		Midday trough		Evening peak		Morning peak		Midday trough		Evening peak	
Geomagnetic classes of activity	Local time	foF2 (MHz)	Local time	foF2 (MHz)	Local time	foF2 (MHz)	Local time	foF2 (MHz)	Local time	foF2 (MHz)	Local time	foF2 (MHz)
Quiet	9	11.51	11	11.03	16	12.54	10	13.33	14	12.40	16	13
Fluctuating	10	12.68	12	11.30	17	12.45	11	14	14	11.85	16	12.35
Recurrent	11	13.50	–	–	–	–	10	12.75	14	11.10	15	11.45
Shock	10	14.67	–	–	–	–	10	15	–	–	–	–
	Summer						Autumn					
	foF2 graph characteristics											
	Sunspot maximum											
	Morning peak		Midday trough		Evening peak		Morning peak		Midday trough		Evening peak	
Geomagnetic classes of activity	Local time	foF2 (MHz)	Local time	foF2 (MHz)	Local time	foF2 (MHz)	Local time	foF2 (MHz)	Local time	foF2 (MHz)	Local time	foF2 (MHz)
Quiet	10	11.87	14	10.63	18	11	10	9.44	12	8.48	18	11.54
Fluctuating	11	12.63	15	11.02	18	11.70	11	12.25	16	10.20	17	10.67
Recurrent	13	11.44	–	–	–	–	10	13	13	11	16	12.20
Shock	10	11	11	10.20	17	11.70	10	13.30	15	10.53	17	11.07

Table 4. Characteristics of the observations of foF2, (a) for the sunspot minimum during winter and spring for the four classes of geomagnetic activity, and (b) for the sunspot minimum during summer and autumn for the four classes of geomagnetic activity.

	Winter						Spring					
	foF2 graph characteristics											
	Sunspot minimum											
	Morning peak		Midday trough		Evening peak		Morning peak		Midday trough		Evening peak	
Geomagnetic classes of activity	Local Time	foF2 (MHz)	Local Time	foF2 (MHz)	Local Time	foF2 (MHz)	Local Time	foF2 (MHz)	Local Time	foF2 (MHz)	Local Time	foF2 (MHz)
Quiet	10	7.65	11	7.30	17	7.90	9	8.28	15	8.4	18	9.48
Fluctuating	9	7.25	14	7.07	17	8.08	9	8.78	10	8.28	17	10
Recurrent	9	8.33	13	7.37	16	8.83	9	8.39	15	8.49	18	9.4
Shock	10	8.86	12	7.55	18	9.5	11	11	15	9	18	12
	Summer						Autumn					
	foF2 graph characteristics											
	Sunspot minimum											
	Morning peak		Midday trough		Evening peak		Morning peak		Midday trough		Evening peak	
Geomagnetic classes of activity	Local time	foF2 (MHz)	Local time	foF2 (MHz)	Local time	foF2 (MHz)	Local time	foF2 (MHz)	Local time	foF2 (MHz)	Local time	foF2 (MHz)
Quiet	8	7	12	6.74	17	8.64	9	7.8	12	6.86	17	8.84
Fluctuating	10	7.33	14	6.40	18	7.52	10	8.96	12	8.56	17	10.9
Recurrent	9	6.95	12	6.58	17	8.63	10	10.75	16	9	17	11.5
Shock	10	7.80	12	7.40	17	9.50	10	8.95	12	8.40	16	9.75

(Table 3b) whatever the magnetic activity, all foF2 morning peaks roughly present the same amplitude. The morning peak time changes with the season and the magnetic activity between 09:00 LT and 13:00 LT. The midday trough is observed earlier in winter than in the other seasons. Between 15:00 LT and 18:00 LT the location of the evening peak also changes with season and magnetic activity.

Tables 4a and 4b give for the sunspot minimum and during the four seasons, foF2 peak and trough values and locations. At sunspot minimum for all magnetic classes and all seasons there is always the same pattern: morning peak, midday trough and evening peak. The amplitude of the evening peak is always greater than that of the morning one. The highest values of the evening peak are observed in spring under shock condition (12 MHz) and in autumn under recurrent condition (11.5 MHz).

During sunspot minimum, foF2 amplitudes for the different magnetic classes and different seasons are not scattered as much as during sunspot maximum.

5. Summary and conclusion

Our results confirm the well-known characteristics of the foF2 frequencies (good correlation between foF2 and sunspot number, and how foF2 reacts under geomagnetic storm conditions. For example, the variation of the amplitude related to the sunspot solar cycle (toroidal component of the solar magnetic field), and the positive and the negative magnetic storms in relation to geomagnetic conditions (recurrent and shock conditions).

This statistical analysis shows three main patterns:

1. The regular pattern with morning peak, midday trough and evening peak mainly related to quiet and fluctuating activities (Figs. 1b, 2a, 2b, 4a, 4b, 5a and 5b). The same pattern was observed by Obrou et al. (2009) on the diurnal variation of the TEC estimated with the ionosonde of Korhogo located near Ouagadougou.
2. An irregular pattern with one peak in the morning or one peak in the afternoon (Figs. 1a, 3a and 6a) mainly related to the shock or recurrent activity at sunspot maximum.
3. An unclear pattern for recurrent and shock activities during sunspot minimum (Figs. 3b and 6b).

This statistical analysis also shows the seasonal asymmetry between the increasing and the decreasing phases of sunspot cycle for quiet activity (Figs. 4a and 4b). During the increasing phase, spring and autumn show the highest foF2, and during the decreasing phase of the sunspot cycle, the highest values of the foF2 are observed in spring and summer.

Our observations show a great seasonal scattering of the observations during the sunspot maximum for the recurrent, quiet, shock activities (Figs. 1a, 3a, 4a and 6a) and during the sunspot minimum for the recurrent and shock activities (Figs. 3b and 6b).

Concerning the fluctuating activity, the observations exhibit similar patterns for the increasing and decreasing phases (Figs. 5a and 5b), but these patterns do not correspond to the signature of a particular solar event.

Our results show the importance of studying long series of both ionospheric and solar data; indeed, such databases allow for a better understanding of the variability of the diurnal variation of the F2 critical frequencies. The empirical model presented in this paper gives 64 diurnal variations of the foF2 layer depending on the season, the sunspot solar cycle the speed of the solar wind and shock activities (these last two parameters are at the origin of geomagnetic activity). These diurnal variations may be of help in determining the morphological behaviour of each class of activity in the equatorial region; and certainly in West Africa where there is a lack of long series of ionospheric data.

We found that the signatures of the different classes of solar activities (1) recurrent activity/high wind streams, (2) shock activity, (3) quiet (slow solar wind) and (4) fluctuating (fluctuating solar wind) activities are clearly identified on the diurnal pattern of the foF2 critical frequency. The precise empirical dependencies on these conditions suggest that physical mechanisms are needed for full future theoretical interpretation.

From GPS data, we can derive F2 layer frequency and therefore pursue this work. In the future, we will also consider more active (sunspot number > 100) and weaker (sunspot number < 100) as the actual solar cycle. It will also be possible to add new classes taking into account physical disturbed processes acting in the Sun-Earth system during magnetic storms, such as meridional thermospheric winds at F region heights produced by Joule heating in the auroral zone (Testud & Vasseur 1969; Richmond & Roble 1979), changes in the atmospheric composition (Jones 1971; Jones & Risbeth 1971; Volland 1979), prompt penetration of the magnetospheric convection electric field (Vasyliunas 1970) or the disturbance dynamo electric field (Blanc & Richmond 1980). At low latitudes within ±20° dip latitude, the E × B vertical drift is the primary cause of the redistribution of the ionospheric plasma. During magnetically disturbed periods the equatorial electric field is affected by prompt penetration of the magnetospheric convection and/or the ionospheric disturbance dynamo. In the past, many studies were made on the electric field parameter during quiet magnetic periods and these studies showed seasonal, solar cycle, latitudinal and longitudinal variations in this parameter (Fejer et al. 1979, 1991; Richmond et al. 1980; Scherliess & Fejer 1999). Studies were also made during magnetically disturbed periods (Fejer & Scherliess 1997), but all the studies did not include electric field measurements due to the lack of data in Africa. Recently Shim et al. (2010) made an extensive study on the effects of the neutral wind and plasma drifts on low and middle latitude ionization using TEC measurements (comparable to foF2). They found that ionization can increase or decrease under the effect of neutral wind or plasma drift, but the response vary with the hemisphere, with the longitude and also with the local time of the disturbance. Therefore, it seems necessary to develop comparisons with models adapted to our classification and Africa. This is the scope of another paper.

In summary

1. The present work gives a detailed description of the mean foF2 diurnal variation at Ouagadougou over three solar cycles.
2. It allows us to illustrate the shape of the mean diurnal foF2 variation as a function of season, solar activity (sunspot solar cycle), solar wind and shock event (geomagnetic activity). The toroidal component of the solar magnetic field causes the large variation in the diurnal amplitude of the F2 layer frequency, while the poloidal component of the solar magnetic field and the shock events mainly influence the shape of foF2. With such approach, it is possible to relate the F2 layer critical frequency (foF2) to the two large-scale components of the solar magnetic field, in order to extend Geophysics to Heliophysics.
3. Our discussion provides starting points for further theoretical research.

Our results are revealing a large amount of new facts. This makes our work useful for future model studies of the complex equatorial F2 layer behaviour. This will also allow new theoretical studies of the equatorial atmosphere.

With the increase of database all over the planet it will soon be possible to develop empirical statistical models of ionospheric parameters taking into account detailed solar conditions and physical processes acting in the Sun-Earth system and later to predict in real time the impact of the Sun on ionization by using large existing databases: this is the goal of scientific programmes such as ISWI (International Space Weather Initiative). In this programme many scientific instruments are deployed over Africa in order to overcome the lack of data for this continent.

Acknowledgements. The authors thank Paul Vila for his comments and corrections. The authors thank the CNET institution which collected and processed the data during 32 years. The authors also thank Rolland Fleury and Patrick Lassudrie Duchesne for providing Ouagadougou Ionosonde data. Many thanks to reviewers for their suggestions, remarks, advice and proofreading.

References

Amory-Mazaudier, C., M. Le Huy, Y. Cohen, V. Doumouya, A. Bourdillon, et al., Sun-Earth system interactions over Vietnam: An international cooperative project, *Ann. Geophys.*, **24**, 3313–3327, 2006.

Arauje-Pradere, E.A., foF2 frequency bands in el Cerrillo, Mexico during magnetically quiet conditions, *Rev. Bras. Geofis.*, **15 (2)**, 161–164, 1997.

Blanc, M., A. Richmond, The ionospheric Disturbance Dynamo, *J. Geophys. Res.*, **85**, 1669–1686, 1980.

Breit, G., and M.A. Tuve, Test of the existence of the conducting layer, *Phys. Rev.*, **28**, 554–575, 1926.

Burns, A.G., T.L. Killeen, and R.G. Roble, A simulation of thermospheric composition changes during an impulsive storm, *J. Geophys. Res.*, **96**, 14153–14167, 1991.

Burns, A.G., T.L. Killeen, G.R. Carignan, and R.G. Roble, Large enhancements in the O/N2 ratio in the evening sector of the winter hemisphere during geomagnetic storms, *J. Geophys. Res.*, **100**, 14661–14671, 1995.

Fejer, B., D.T. Farley, R.F. Woodman, C. Calderon, Dependence of Equatorial F region Vertical Drifts on Season and Solar Cycle, *J. Geophys. Res.*, **84 (A10)**, 5792–5796, 1979.

Fejer, B., E.R. Paula, S.A. Gonzalez, S.A. Gonzalez, R.F. Woodman, Average vertical and zonal F region plasma drifts over Jicamarca, *J. Geophys. Res.*, **96 (A8)**, 13901–13906, 1991.

Fejer, B., and L. Scherliess, Empirical model of storm time equatorial zonal electric field, *J. Geophys. Res.*, **102 (A11)**, 24047–24056, 1997.

Fejer, B.G., J.W. Jensen, T. Kikuchi, M.A. Abdu, J.L. Chau, Equatorial ionospheric electric fields during the November 2004 magnetic storm, *J. Geophys. Res.*, **112**, A10304, DOI: 10.1029/2007JA012376, 2007.

Fejer, B.G., Low latitude ionospheric electrodynamics, *Space Sci. Rev.*, **158 (1)**, 145–166, 2011.

Forbes, J.M., S.E. Palo, X. Zhang, Variability of the ionosphere, *J. Atmos. Sol. Terr. Phys.*, **62**, 685–693, 2000.

Huang, C.-S., J.C. Foster, and M.C. Kelley, Long-duration penetration of the interplanetary electric field to the low-latitude ionosphere during the main phase of magnetic storms, *J. Geophys. Res.*, **110**, A11309, DOI: 10.1029/2005JA011202, 2005.

Huang, C.-S., S. Sazykin, J.L. Chau, N. Maruyama, and M.C. Kelley, Penetration electric fields: Efficiency and characteristic time scale, *J. Atmos. Terr. Phys.*, **69 (10–11)**, 1135–1146, 2007.

Jones, K.L., Storm time variation of the F2 layers electron concentration, *J. Atmos. Terr. Phys.*, **33**, 379–389, 1971.

Jones, K.L., H. Risbeth, The origin of storm increases of mid-latitude F-layer electron concentration, *J. Atmos. Terr. Phys.*, **33**, 391–401, 1971.

Lal, C., Global F2 layer ionization and geomagnetic activity, *J. Geophys. Res.*, **97 (A8)**, 12153–12159, 1992.

Lal, C., Contribution to F2 layer ionization due to solar wind, *J. Atmos. Sol. Terr. Phys.*, **99 (17)**, 2203–2211, 1997.

Lal, C., Contribution of Solar wind and equinoctial maxima in geophysical phenomena, *J. Atmos. Sol. Terr. Phys.*, **60**, 1017–1024, 1998.

Legrand, J.P, and P.A. Simon, Solar cycle and geomagnetic activity: A review for geophysicists. Part I. The contributions to geomagnetic activity of shock waves and of the solar wind, *Ann. Geophys.*, **7 (6)**, 565–578, 1989.

Lotko, W., Report of the working group on ionospheric signatures. GEM report on the Workshop on Magnetospheric and Boundary Layer Physics, La Jolla, CA, 1989.

Lu, G., A.D. Richmond, R.G. Roble, and B.A. Emery, Coexistence of ionospheric positive and negative storm phases under northern winter conditions: A case study, *J. Geophys. Res.*, **106**, 24493–24504, 2001.

Manoj, C., S. Maus, H. Lühr, and P. Alken, Penetration characteristics of the interplanetary electric field to the daytime equatorial ionosphere, *J. Geophys. Res.*, **113**, A12310, DOI: 10.1029/2008JA013381, 2008.

Nicolls, M.J., M.C. Kelley, J.L. Chau, O.Veliz, D. Anderson, and A. Anghel, The spectral properties of low latitude daytime electric fields inferred from magnetometer observations, *J. Atmos. Terr. Phys.*, **69 (10–11)**, 1160–1173, 2007.

Obrou, O.K., M.N. Mene, A.T. Kobea, and K.Z. Zaka, Equatorial Total Electron Content (TEC) at low and high solar activity, *Adv. Space Res.*, **43 (11)**, 1757–1761, 2009.

Ouattara, F., Contribution à l'étude des relations entre les deux composantes du champ magnétique solaire et l'ionosphère équatoriale, *UCAD*, 340 p, 2009a.

Ouattara, F., Relationship between geomagnetic classes' activity phases and their occurrence during the sunspot cycle, *Ann. Geophys.*, **52 (2)**, 107–116, 2009b.

Ouattara, F., and C. Amory Mazaudier, *J. Atmos. Terr. Phys.*, **71**, 1736–1748, 2009.

Ouattara, F., C. Amory Mazaudier, P. Vila, R. Fleury, and P. Lassudrie Duchesne, West African equatorial ionospheric parameters climatology based on Ouagadougou station Ionosonde data from June 1966 to February 1998, *Ann. Geophys.*, **27**, 2503–2514, 2009.

Pancheva, D., N. Mitchell, R.R. Clark, J. Drobjeva, and J. Lastovicka, Variability in the maximum height of the ionospheric F2-layer over Millstone (September 1998–March 2000); influence from below and above, *Ann. Geophys.*, **20 (11)**, 1807–1819, 2002.

Phillips, M.L., The ionosphere as a measure of solar activity, *Terr. Mag. Atmos. Electr.*, **52 (3)**, 321–332, 1947.

Prölss, G.W., Storm-induced changes in the thermospheric composition at middle latitudes, *Planet. Space Sci.*, **35**, 807–811, 1987.

Ren, Z., W. Wan, L. Liu, and J. Xiong, Intra-annual variation of wave number-4 structure of vertical ExB drifts in the equatorial ionosphere seen from ROCSAT-1, *J. Geophys. Res.*, **114**, A05308, DOI: 10.1029/2009JA014060, 2009.

Richardson, I.G., E.W. Cliver, and H.V. Cane, Sources of geomagnetic activity over the solar cycle: Relative importance of coronal mass ejections, high-speed streams, and slow solar wind, *J. Geophys. Res*, **105**, 18200–18213, 2000.

Richmond, A., M. Blanc, B.A. Emery, R-H. Wand, B.G. Fejer, et al., *J. Geophys. Res.*, **85 (A8)**, 4658–4664, 1980.

Richmond, A., and R.G. Roble, Dynamic effects of aurora generated gravity waves on mid-latitude ionosphere, *J. Atmos. Terr. Phys.*, **41**, 841–852, 1979.

Rishbeth, H., F-region storms and thermospheric circulation, in *Electromagnetic Coupling in the Polar Clefts and Caps*, eds. P.E., Sandholt, and A. Egeland, Kluwer Academic, Norwell, MA, pp. 393–406, 1989.

Rishbeth, H., and M. Mendillo, Pattern of F2-layer variability, *J. Atmos. Sol. Terr. Phys.*, **63**, 1661–1680, 2001.

Rishbeth, H.I., C.F. Müller-Wodarg, L. Zou, T.J. Fuller-Rowell, G.H. Millward, R.J. Moffett., D.W. Idenden, and A.D. Aylward, Annual and semiannual variations in the ionospheric F2-layer: II. Physical discussion, *Ann. Geophys.*, **18**, 945–956, 2000.

Scherliess, L., and B.G. Fejer, Radar and satellite global equatorial E region vertical drift model, *J. Geophys. Res.*, **104**, 6829–6842, 1999.

Shim, J.S., L. Scherliess, R.W. Shink, and D.C. Thomspon, Neutral wind and plasma drift effects on low and middle latitudes total electron content, *J. Geophys. Res.*, **115**, A04307, DOI: 10.1029/2009JA014488, 2010.

Simon, P.A., and J.P. Legrand, Solar cycle and geomagnetic activity: A review for geophysicists. Part II. The solar sources of geomagnetic activity and their links with sunspot cycle activity, *Ann. Geophys.*, **7 (6)**, 579–594, 1989.

Testud, J., and G. Vasseur, *Ondes de gravité dans la thermosphere*, *Ann. Geophys.*, **25**, 525–546, 1969.

Vasyliunas, V.H., A mathematical model of magnetospheric convection and its coupling to the ionosphere, in *Particles and Fields in the Magnetosphere*, eds. B.M., Cormac, and D. Reidel, vol. **60**, Hollant, 1970.

Volland, H., Magnetospheric Electric Fields and Currents and their influence on large scale thermospheric circulation and composition, *J. Atmos. Sol. Terr. Phys.*, **41**, 853–866, 1979.

Zou, L., H.I. Rishbeth, C.F. Müller-Wodarg, A.D. Aylward, G.H. Millward, T.J. Fuller-Rowell, D.W. Idenden, and R.J. Moffett, Annual and semiannual variations in the ionospheric F2-layer: I. Modelling, *Ann. Geophys.*, **18**, 927–944, 2000.

View publication stats